Supplementary Information

Investigating the detection limit of subsurface holes under graphite with atomic force acoustic microscopy

Kevin Yip,[a] Teng Cui,[a] Yu Sun,[a] and Tobin Filleter[*a]

[a] *Department of Mechanical and Industrial Engineering, University of Toronto, 5 King's College Rd, Toronto, ON, Canada, M5S 3G8*

[*] *Corresponding author*

S1. Thickness Measurements of Various Graphite Flakes

All thickness measurements were taken with the AFM and the following Fig. S1 shows the height line scans of the various graphite flakes used throughout the manuscript.

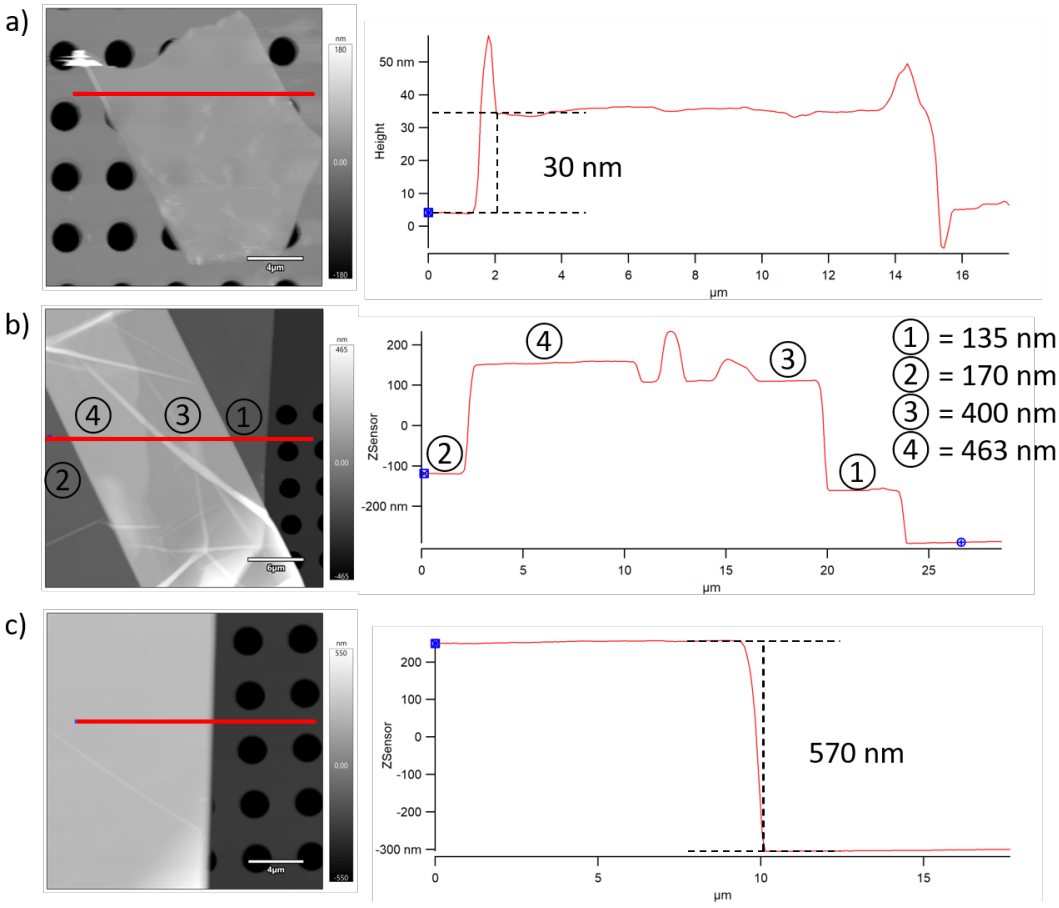

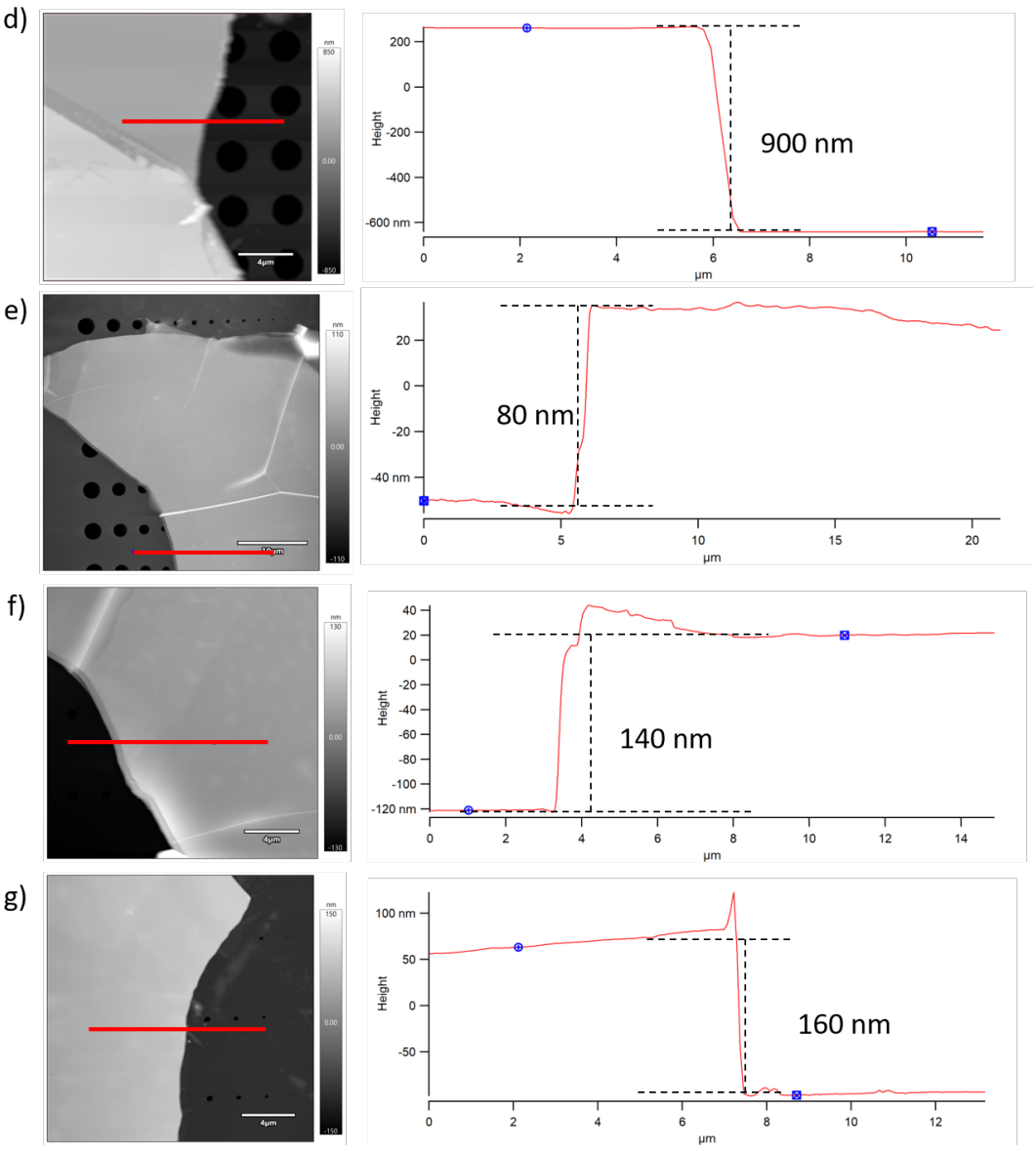

Figure S1: AFM topography and corresponding line profile of various graphite flakes. a) 30 nm flake showing some contrast of buried 2.5 µm holes. b) Graphite flake ranging from 135 - 463 nm over 2.5 µm holes. c) 570 nm thick graphite flake over 2.5 µm holes. d) 900 nm thick graphite flake over 2.5 µm holes. e) 80 nm thick graphite flake suspending over decreasing hole sizes from 2.5 µm holes. f) 140 nm thick graphite flake suspended over decreasing hole sizes. g) 160 nm thick graphite flake suspended over decreasing hole sizes.

S2. AFAM Experimental Setup

The AFAM technique as described by Rabe et al.,[1] utilizes a piezoelectric transducer placed beneath the sample to emit acoustic vibrations which is then picked up by the AFM cantilever. A custom piezoelectric transducer was built to perform this technique. A piezo disk with a resonance frequency of 1 MHz was purchased from Physik Instrument (PRYY +0372) and copper contacts were glued on both sides of the disk with a silver epoxy (Epotek H20E)[2]. A BNC cable was used to apply the drive voltage and frequency to the piezoelectric transducer. The sample was then glued to the top of the piezoelectric stage with phenyl salicylate[3].

The technique was carried out with the Asylum MFP-3D, where a built in technique allowed us to determine the contact resonance frequency of the cantilever while it is in contact with the surface. A signal is sent to the piezoelectric transducer and the spectral components of the cantilever is recorded, displaying the various contact eigenmodes. To perform the subsurface AFAM imaging, we utilized a mode which allowed us to image in contact mode with a constant contact force while applying a drive frequency to the custom piezoelectric transducer the sample was sitting on. The topography, amplitude, and phase were recorded simultaneously. As the feedback loop in this mode was maintaining the contact force rather than the cantilever amplitude (as in tapping mode), the cantilever oscillation varied and is displayed in the amplitude channel as it scans over the surface.

S3. Signal-to-noise and Amplitude Change Calculations

The following Fig. S2 shows the calculations for obtaining signal-to-noise and amplitude change that is present in Fig. 2, 4 - 7 in the manuscript, as well as in Fig. S3.

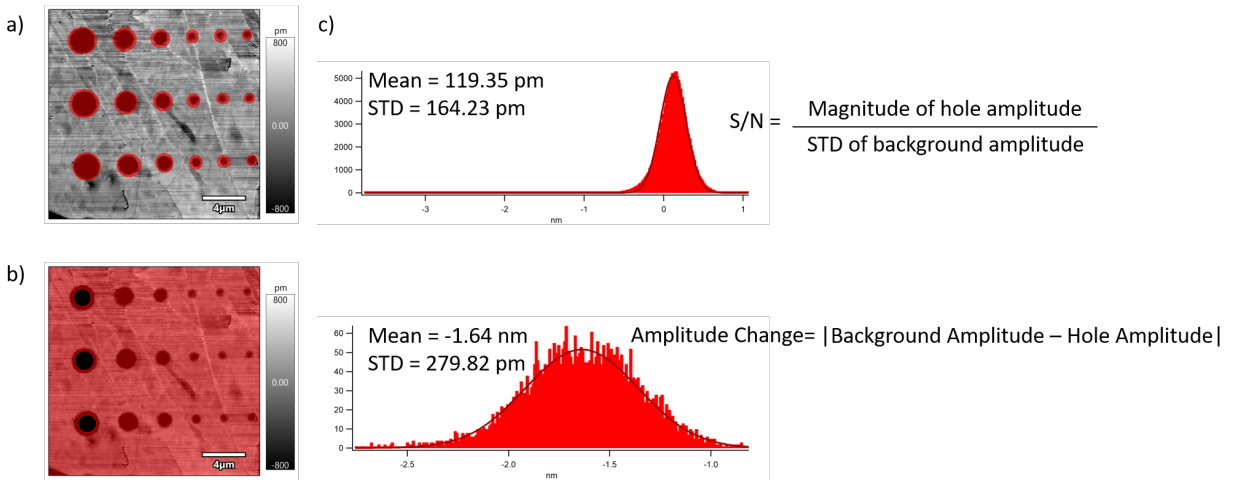

Figure S2: a) Masks corresponding to background graphite amplitude and b) hole amplitude. c) Histograms of the background graphite amplitude (upper) and hole amplitude (lower). Determination of both S/N and amplitude change using the given histograms

In Fig. S2, the red mask corresponds to the removal of unwanted data points. Fig. S2a is taking only the background graphite amplitude to obtain the mean and standard deviation while Fig. S2b is only looking at the 2.5 µm hole amplitude. To determine the S/N, the magnitude of the amplitude in the hole is divided by the error (standard deviation) in the background graphite amplitude [4]. The amplitude change is simply the absolute value of the difference between the background graphite amplitude and the hole amplitude.

S4. Effect of Cantilever Stiffness on Subsurface Defect Detection

To study the relationship between cantilever stiffness and subsurface defect detection, three cantilevers with different stiffnesses were used at the same contact force of 110 nN. The cantilevers had a stiffness of 1.13 N/m (D160), 2.89 N/m (ASYELEC), and 21.80 N/m (NCLR). The drive frequencies for all cantilevers were 10 - 20 kHz above the contact resonance. The following Fig. S3 shows the resulting S/N and amplitude changes of the different stiffnesses at various hole sizes.

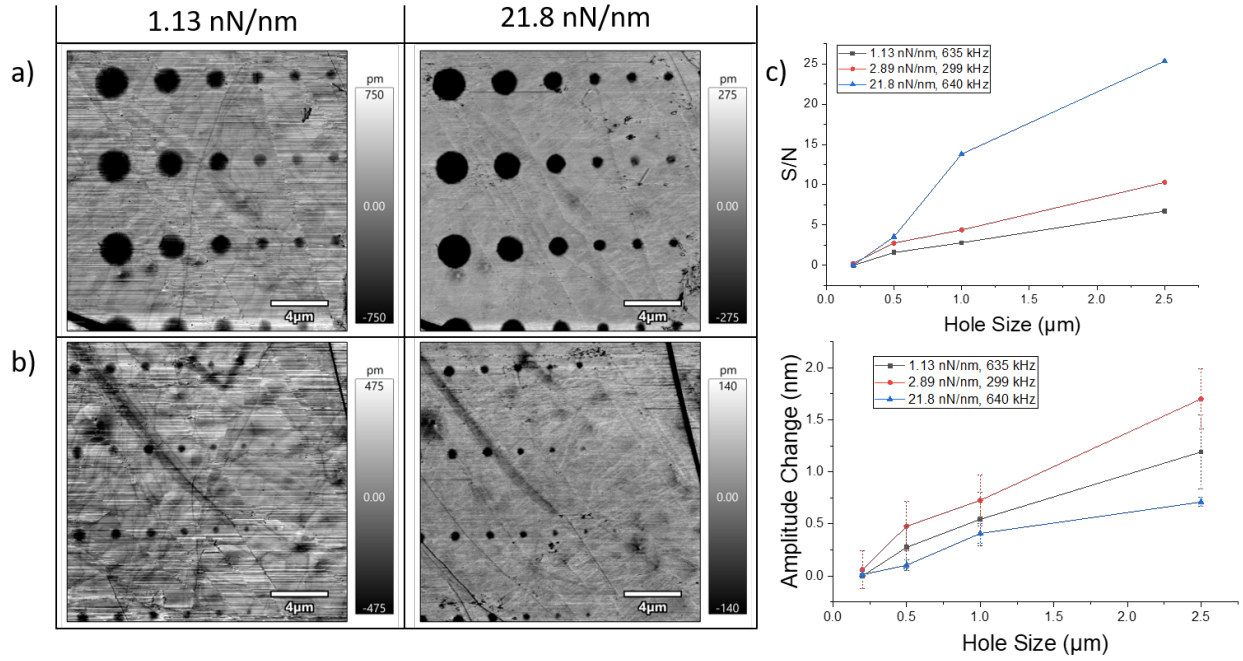

Figure S3: a) AFAM amplitude images at 1.13 nN/nm and 21.8 nN/nm, featuring hole sizes from 2.5 µm - 800 nm and b) 900 nm - 100 nm. c) Signal-to-noise ratio of the various hole sizes at different stiffnesses and the corresponding amplitude change

While the S/N ratio is improved on the larger hole sizes using stiffer cantilevers, it does not have a significant effect on smaller holes. Similar to varying contact force and using higher eigenmodes, the smallest detectable hole size was 100 nm for all stiffnesses.

References

[1] U. Rabe and W. Arnold, "Acoustic microscopy by atomic force microscopy," *Applied Physics Letters*, vol. 64, no. 12, pp. 1493–1495, 1994.

[2] G. J. Verbiest, D. J. Van Der Zalm, T. H. Oosterkamp, and M. J. Rost, "A subsurface add-on for standard atomic force microscopes," *Review of Scientific Instruments*, vol. 86, no. 3, 2015.

[3] K. Yamanaka, "UFM observation of lattice defects in highly oriented pyrolytic graphite," *Thin Solid Films*, vol. 273, no. 1-2, pp. 116–121, 1996.

[4] K. Kimura, K. Kobayashi, K. Matsushige, and H. Yamada, "Imaging of Au nanoparticles deeply buried in polymer matrix by various atomic force microscopy techniques," *Ultramicroscopy*, vol. 133, pp. 41–49, 2013.